

Search for Decays of the ${}^9\text{B}$ Nucleus and Hoyle State in ${}^{14}\text{N}$ Nucleus Dissociation

E. Mitsova^a, A. A. Zaitsev^{a, *}, D. A. Artemenkov^a, N. K. Kornegrutsa^a, V. V. Rusakova^a,
R. Stanoeva^b, P. I. Zarubina^a, and I. G. Zarubina^a

^a Joint Institute for Nuclear Research, Dubna, 141980 Russia

^b Southwestern University, Blagoevgrad, Bulgaria

*e-mail: zaitsev@lhe.jinr.ru

Received March 11, 2021; revised July 8, 2021; accepted July 18, 2021

Abstract—The first results on analysis of determination of the contribution of decays of unstable ${}^8\text{Be}$ and ${}^9\text{B}$ nuclei and the Hoyle 3α -state into the dissociation of ${}^{14}\text{N} \rightarrow 3\text{He} (+\text{H})$ are presented. Layers of nuclear track emulsion longitudinally exposed to $2.9 A \text{ GeV}/c$ ${}^{14}\text{N}$ nuclei at the JINR Nuclotron are used as the research material. Under the assumption that He and H fragments preserve momentum per nucleon of the primary nucleus, these unstable states are identified by the minimum invariant mass calculated using fragment emission angles.

DOI: 10.1134/S1063779622020575

INTRODUCTION

In the limiting fragmentation region, the value of primary energy or the target composition do not affect the manifestation of cluster properties of studied nuclei. The investigation via nuclear track emulsion (NTE) of the composition of relativistic dissociation of light nuclei in the BECQUEREL experiment indicates the contribution of decays of unstable ${}^8\text{Be} \rightarrow 2\alpha$ and ${}^9\text{B} \rightarrow {}^8\text{Be}p$ nuclei, as well as 3α -decay of the Hoyle state (HS) [1, 2]. Along with its identification in the relativistic dissociation of the ${}^{12}\text{C}$ nucleus, the HS was manifested in the case of ${}^{16}\text{O}$ as an unstable 3α -nucleus similar to ${}^8\text{Be}$. According to the widths for ${}^8\text{Be}$ (5.6 eV), ${}^9\text{B}$ (540 eV), and HS (9.3 eV) [3], their decays take place during times exceeding by several orders of magnitude the time of relativistic reaction. The minimum decay energy for ${}^8\text{Be}$ (92 keV), ${}^9\text{B}$ (185 keV), and HS (378 keV) [3] is manifested in the smallest opening angles of the pairs and triplets of He and H fragments, partializing them on the background of other fragmentation products.

The invariant mass of the system of relativistic fragments is determined as the sum of all products of 4-momenta $P_{i,k}$ for the fragments $M^{*2} = \sum(P_i P_k)$. Subtraction of the mass of the sum of fragment masses $Q = M^* - M$ is convenient for representation. The components $P_{i,k}$ are determined in the approximation of conservation of initial momentum per nucleon by fragments. It is often sufficient to assume the correspondence $\text{He}-{}^4\text{He}$ and $\text{H}-{}^1\text{H}$, since in the case of stable nuclei established contributions of ${}^3\text{He}$ and ${}^2\text{H}$ do not

exceed 10%. This simplification used hereinafter is especially valid in the case of extremely narrow ${}^8\text{Be}$ and ${}^9\text{B}$ decays. In the assumption of conservation of momentum per nucleon of the primary nucleus by fragments, unstable states are identified by the minimum invariant mass calculated using He and H fragments emission angles. Then for their selection, it is sufficient to introduce a limit of several hundred keV on the invariant mass of final fragment pairs and triplets (minus the total mass of the latter fragments).

Being independent of initial energy and multiplicity of dissociation, the developed approach allows one to study the role of unstable nuclei as elements of the cluster structure of light nuclei in a unified way. Moreover, it becomes possible to search for nuclear-molecular states with electromagnetic widths, such as ${}^9\text{B}p$, ${}^9\text{B}\alpha$, and $\text{HS}p$, products of α particle or proton decay of which may be the HS or ${}^9\text{B}$, and finally ${}^8\text{Be}$. Thus, it becomes possible to “disentangle in the reverse order” cascade decays on the background of other products of nuclear dissociation.

The material for such study may be NTE, longitudinally exposed to ${}^{14}\text{N}$ nuclei with a momentum of $2.9 A \text{ GeV}/c$ at the JINR Nuclotron in 2004. The charge topology of ${}^{14}\text{N}$ dissociation was found earlier, and the contribution of ${}^8\text{Be}$ was estimated as 25–30% [4]. The topical question is the role of ${}^9\text{B}$ and the HS. The ${}^{14}\text{N}$ nucleus, along with ${}^{10}\text{B}$, belongs to an extremely small number of stable odd–odd nuclei (note also ${}^2\text{H}$, ${}^6\text{Li}$, ${}^{50}\text{V}$). The cluster pattern of dissociation of these nuclei on the whole and the formation of

unstable nuclei in particular can be similar. The data on dissociation of ^{10}B nucleus obtained based on irradiation at Nuclotron in 2002 give the closest possibility for verification and comparison [5]. The analysis in this direction is given below.

SEARCH AND MEASUREMENT OF INTERACTIONS

Fragmentation events were sought during transverse scanning of NTE layers. The observed pairs of He tracks or pairs with the heaviest fragment were traced toward the interaction vertex for finding other tracks. Table 1 gives the distribution of the main statistics over the topology of fragments with the charge Z . Although there exists a difference from the result of event search along primary tracks [4], the main branch of statistics $^{14}\text{N} \rightarrow 3\text{He}$ is observed with the same efficiency. An example of event of coherent dissociation $^{14}\text{N} \rightarrow 3\text{HeH}$ (“white” star) not accompanied by produced mesons and target fragments in a wide cone is shown in Fig. 1. A small number of white 3α -stars, attributed to the admixture of ^{12}C nuclei in the beam was not included in the statistics.

The statistics of the 3HeH dissociation channel, which is of the main interest, is the leading one both among white stars $N_{\text{ws}}(3\text{HeH})$ and interactions with target fragments $N_{\text{tf}}(3\text{HeH})$. For events with 3HeH and 3He fragments, which look like neutron or proton stripping with target destruction, there is a substantial difference in the numbers of N_{tf} . Their ratio is $N_{\text{tf}}(3\text{HeH})/N_{\text{tf}}(3\text{He}) = 1.9 \pm 0.2$. A similar channel 2HeH of ^{10}B isotope dissociation, also the leading one, was represented by the number of stars of both types, $N_{\text{ws}}(2\text{HeH}) = 103$ (76% N_{ws}) and $N_{\text{tf}}(2\text{HeH}) = 182$ (48% N_{tf}), and their ratio is $N_{\text{tf}}(2\text{HeH})/N_{\text{tf}}(2\text{He}) = 182/89$ or 2.1 ± 0.3 [5]. These relations can be used for

Table 1. Distribution of “white” stars N_{ws} and peripheral interactions with the target fragments N_{tf} over the number of relativistic fragments N_Z with the charge Z

ΣZ	6		7			
$N_{Z>2}$	–	–	1	–	–	–
$N_{Z=2}$	3	2	2	2	3	3
$N_{Z=1}$	–	2	–	3	1	–
N_{ws}	11	9	9	16	59	–
N_{tf}	90	138	11	81	167	90

verification of detailed calculation of the structure of these nuclei.

The planar and depth angles of tracks from relativistic fragments were measured for reconstruction of decays of unstable nuclei using the highest precision coordinate method on the described statistics. At present, the measurements are performed in 60 3HeH events, including 14 white stars, and 20 3He events with tracks in a wide cone. Polar angles of these tracks with respect to the primary θ_{He} and θ_{H} are calculated on the basis of these measurements. Their distributions shown in Fig. 2 are described by the Rayleigh distribution with $\sigma_{\theta_{\text{He}}} = 9.6 \pm 0.5$ mrad and $\sigma_{\theta_{\text{H}}} = 25 \pm 9$ mrad.

IDENTIFICATION OF UNSTABLE STATES

Angular measurements allow one to analyze relative angles between tracks. The distribution of combinations of the pairs of α particles with respect to the relative spatial angle $\Theta_{2\text{He}}$ in $^{14}\text{N} \rightarrow 3\text{He}$ events (including $+H$) is shown in Fig. 3. In the region $\Theta_{2\text{He}} < 6$ mrad, the average value is $\langle \Theta_{2\text{He}} \rangle = 3.2 \pm 0.4$ mrad with RMS equal to 2.2 mrad. According to the distribution, it corre-

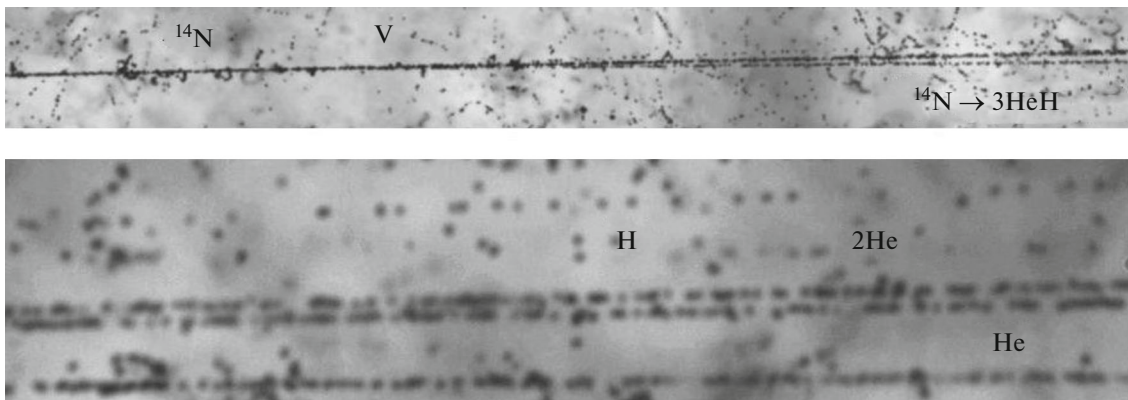


Fig. 1. Macroimage of coherent dissociation of ^{14}N nucleus with a momentum of $2.9 A$ GeV/ c ; the grain size is not larger than $0.5 \mu\text{m}$. The left part of the upper photo shows the primary ^{14}N track accompanied by short δ -electron tracks; the position of the vertex with sharp reduction of ionization is marked (V). For 1 mm along the jet of fragments, their tracks are distinguishable (lower photo); the narrow 2He pair corresponds to ^8Be decay.

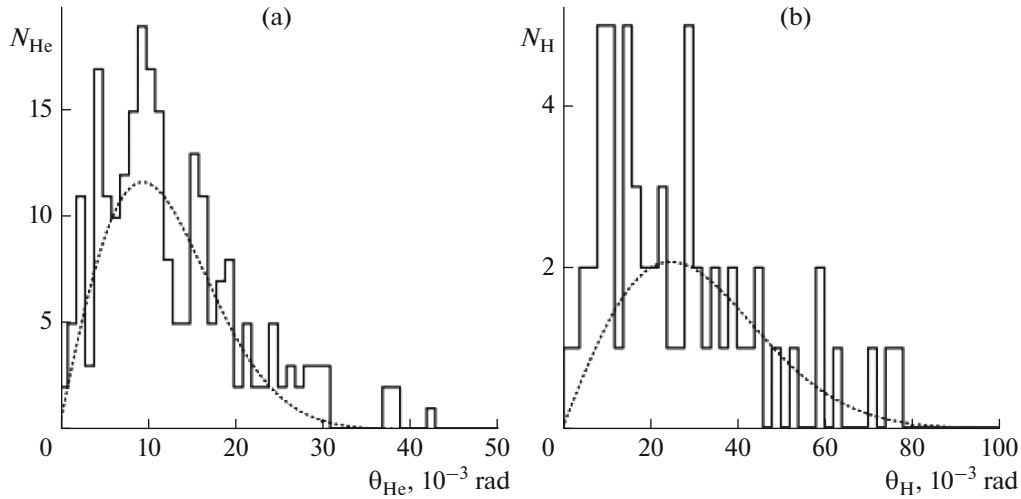


Fig. 2. Distribution of fragments from dissociation $^{14}\text{N} \rightarrow 3\text{He} + \text{H}$ over polar angles (a) θ_{He} and (b) θ_{H} ; points show Rayleigh distribution.

sponds to decays of the ^8Be ground state in the region of smallest values of α -pair invariant mass $Q_{2\alpha}$ (Fig. 4). For 30 events the average value $\langle Q_{2\alpha} \rangle$, satisfying the condition $Q_{2\alpha}(^8\text{Be}) < 0.2$ MeV, was 77 ± 9 keV with RMS equal to 56 keV. Based on it, the contribution of ^8Be nuclei among $^{14}\text{N} \rightarrow 3\text{He}$ events is 38 ± 7 and $45 \pm 9\%$ in $^{14}\text{N} \rightarrow 3\alpha + \text{H}$ channel.

The clustering is observed in the invariant mass distribution of all $2\alpha p$ -triplets for the smallest values of

$Q_{2\alpha}$ (Fig. 5). In the region $Q_{2\alpha p}(^9\text{B}) < 0.5$ MeV the average value $\langle Q_{2\alpha p} \rangle$ for 16 events is 262 ± 28 keV with RMS equal to 120 keV, which allows one to identify them as ^9B decays. The strict condition $Q_{2\alpha}(^8\text{Be}) < 0.2$ MeV reduces their number to 13, which is insignificant. Thus, the contribution of ^9B decays into $^{14}\text{N} \rightarrow 3\alpha p$ dissociation is $22 \pm 9\%$, and into ^8Be decays, $53 \pm 16\%$. This contribution into $^{10}\text{B} \rightarrow 2\alpha p$ dissociation is $8 \pm 2\%$ (26/315) and $45 \pm 11\%$ (26/58), respectively [2].

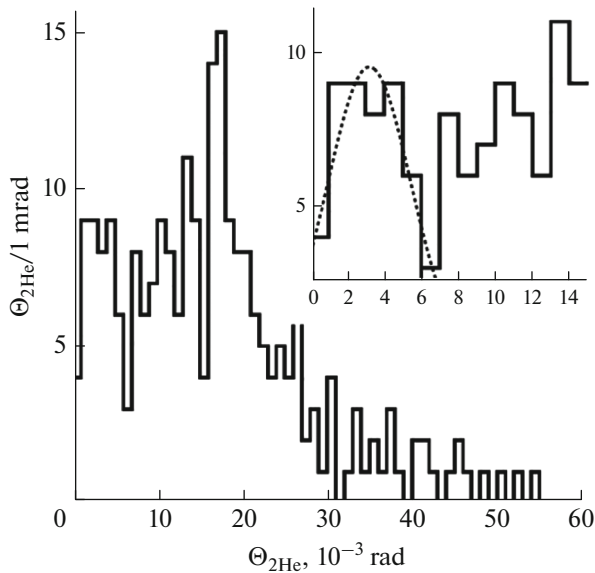


Fig. 3. Distribution over relative spatial angle $\Theta_{2\text{He}}$ for combinations of pairs of α particles in $^{14}\text{N} \rightarrow 3\alpha (+\text{H})$ events; the inset shows the enlarged region of the smallest values of $\Theta_{2\text{He}}$; points show the approximation by the Gaussian function.

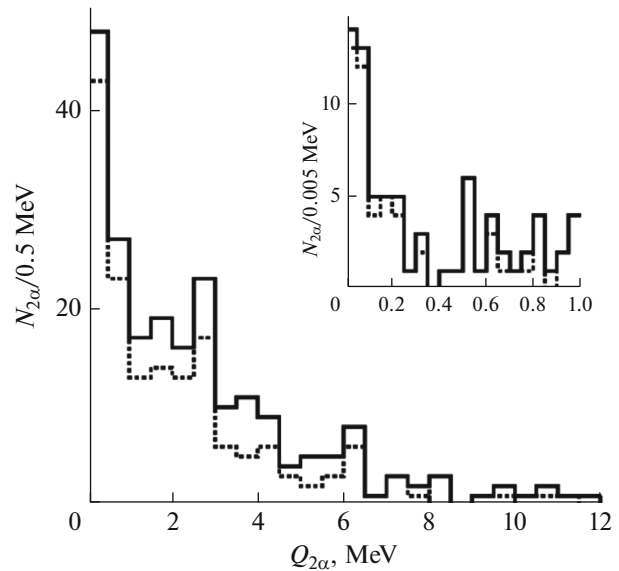


Fig. 4. Invariant mass $Q_{2\alpha}$ distribution for all 2α -pairs in (solid line) $^{14}\text{N} \rightarrow 3\alpha$ events, including (dashed line) 60 $^{14}\text{N} \rightarrow 3\alpha p$ events; the inset shows the enlarged region of the smallest values of $Q_{2\alpha}$.

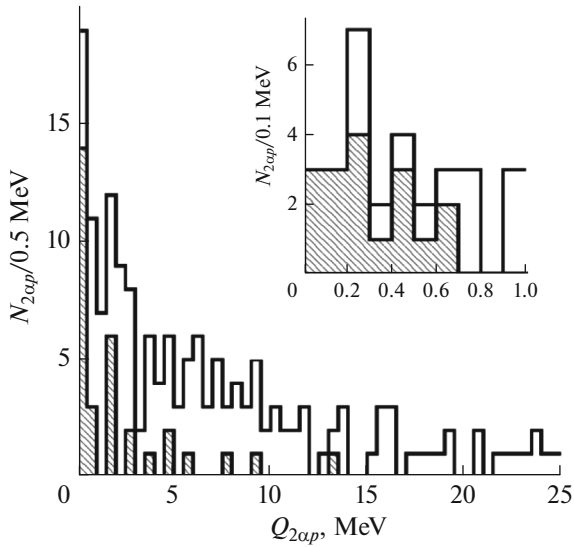


Fig. 5. Invariant mass $Q_{2\alpha p}$ distribution for all $2\alpha p$ -triplets in (solid line) ${}^{14}\text{N} \rightarrow 3\text{HeH}$ events, including (dashed histogram) ${}^{14}\text{N} \rightarrow \alpha^8\text{Be}p$; the inset shows the enlarged region of the smallest values of $Q_{2\alpha p}$.

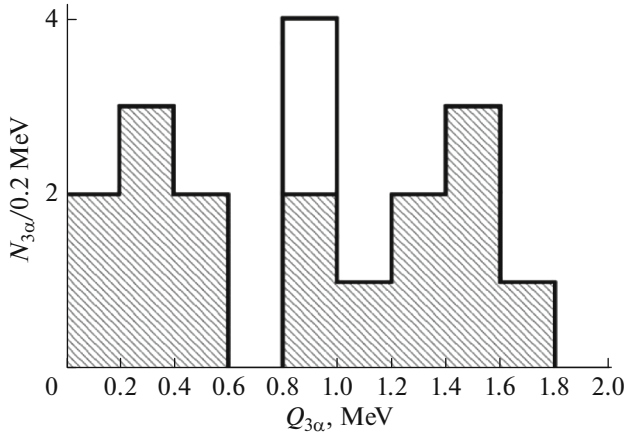


Fig. 6. Distribution in the region of smallest values of invariant mass $Q_{3\alpha}$ for all 3α -triplets in (solid line) ${}^{14}\text{N} \rightarrow 3\text{He}$ events, including (dashed histogram) ${}^{14}\text{N} \rightarrow \alpha^8\text{Be}$.

Note the fact of substantial increase of ${}^9\text{B}$ contribution upon transition from $2\alpha p$ to $3\alpha p$ ensembles with the corresponding increase of $2\alpha p$ combinations with preservation of the ratio of the numbers of ${}^8\text{Be}$ and ${}^9\text{B}$. A similar behavior was noted in investigation of the HS [2]. The rise in the number of 3α -combinations in ${}^{16}\text{O} \rightarrow 4\alpha$ results in the noticeable increase of the contribution of HS decays, and the ratio of ${}^8\text{Be}$ and HS yields is approximately constant.

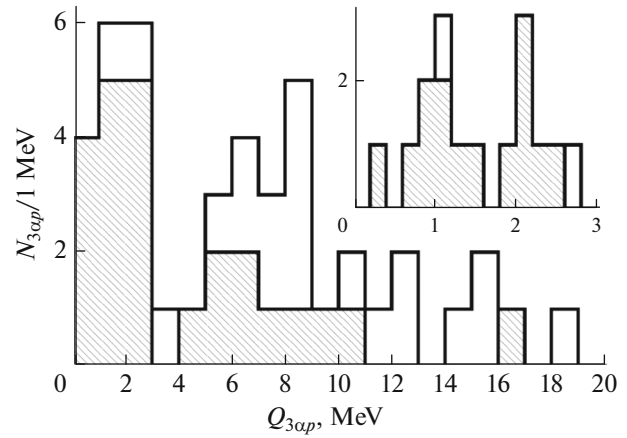


Fig. 7. Invariant mass $Q_{3\alpha p}$ distribution for all $3\alpha p$ -quadruples in (solid line) ${}^{14}\text{N} \rightarrow 3\text{HeH}$ events, including (dashed histogram) ${}^{14}\text{N} \rightarrow \alpha^8\text{Be}p$; the inset shows the enlarged region of the smallest values of $Q_{3\alpha p}$.

In the distribution over invariant mass of all 3α -triplets (Fig. 6), seven events with $\langle Q_{3\alpha} \rangle = 328 \pm 60$ keV with RMS equal to 158 keV satisfy the condition $Q_{3\alpha}(\text{HS}) < 0.7$ MeV. Among these events, two 3HeH events can also be attributed to ${}^9\text{B}$ decays. The contribution of HS decays into ${}^8\text{Be}$ decays is estimated as $23 \pm 10\%$. The small number of $3\alpha p$ -quadruples with the small invariant mass $Q_{3\alpha p}$, although insufficient for discussing a resonance, motivates increasing the statistics (Fig. 7).

CONCLUSIONS

The analysis of dissociation of ${}^{14}\text{N}$ nucleus, as regards the contribution of unstable ${}^8\text{Be}$ and ${}^9\text{B}$ nuclei, is presented. The primary data on the topology of leading channels for both ${}^{10}\text{B}$ and ${}^{14}\text{N}$ nuclei indicate the structural specific features of ${}^{10}\text{B}$ in the leading channel ${}^{14}\text{N} \rightarrow 3\text{He} (+\text{H})$. The contribution of ${}^8\text{Be}$ and ${}^9\text{B}$ to ${}^{14}\text{N}$ dissociation was determined. The new specific feature was the identification of HS decays in the dissociation ${}^{14}\text{N} \rightarrow 3\text{He} (+\text{H})$, which extends the ideas on the universal character of HS earlier established for dissociation of ${}^{12}\text{C}$ and ${}^{16}\text{O}$ nuclei. HS decays correspond to approximately one quarter of ${}^8\text{Be}$ decays not related to ${}^9\text{B}$ decays.

The basis of the topology similarity for dissociation of ${}^{10}\text{B}$ and ${}^{14}\text{N}$ nuclei in the limiting fragmentation region is the similarity of their structural specific features. Approximately equal ratios of the number of events with production of target fragments ${}^{14}\text{N}({}^{10}\text{B}) \rightarrow 3(2)\text{He}$ are determined in a universal way by knocking out external neutrons and protons. The spatial distri-

bution of external neutrons for both nuclei is broader by a factor of two than that of external protons.

Note that ${}^9\text{B}$ decays correspond to not more than one half of ${}^8\text{Be}$ decays, and their ratio is approximately the same in the leading channels ${}^{14}\text{N}({}^{10}\text{B}) \rightarrow 3(2)\text{HeH}$. In the case of coherent dissociation of ${}^{10}\text{C} \rightarrow 2\alpha 2p$ the coincidence of ${}^8\text{Be}$ and ${}^9\text{B}$ decays was complete, and their contribution was 30% [1]. An unexpectedly large ratio of the probability of coherent dissociation of ${}^{10}\text{B}$ into mirror channels ${}^9\text{Bn}$ and ${}^9\text{Bep}$, which made 6 ± 1 , was found earlier [6]. It seems that the ${}^9\text{Be}$ nucleus in the ground state is absent as an ingredient of ${}^{10}\text{B}$ and ${}^{14}\text{N}$, and the sparse nuclear-molecular structure ${}^8\text{Ben}$ is present instead. At the same time, the ground state of ${}^9\text{B}$ represents such a structure initially. Being bound, ${}^8\text{Be}$ nucleus plays the role of the basis in both cases. Assigning half of ${}^8\text{Be}$ decays to the structure ${}^8\text{Ben}$, mirror symmetry could be restored and one could explain why the channels $3(2)\text{He}$ are leading. Since relativistic experiments with neutrons are hardly possible, this hypothesis deserves verification in the low-energy region.

In conclusion, let us note that it is necessary and possible to triply increase the statistics of measured ${}^{14}\text{N} \rightarrow 3\text{He} (+\text{H})$ events, especially as regards the search of resonance $3\alpha p$ states.

CONFLICT OF INTEREST

The authors declare that they have no conflicts of interest.

REFERENCES

1. P. I. Zarubin, “‘Tomography’ of the cluster structure of light nuclei via relativistic dissociation,” *Lect. Notes in Phys.: Clusters in Nuclei* **875** (3), 51 (2014).
2. D. A. Artemenkov, V. Bradnova, M. M. Chernyavsky, E. Firu, M. Haiduc, N. K. Kornegrutsa, A. I. Malakhov, E. Mitsova, A. Neagu, N. G. Peresadko, V. V. Rusakova, R. Stanoeva, A. A. Zaitsev, P. I. Zarubin, and I. G. Zarubina, “Unstable states in dissociation of relativistic nuclei,” *Eur. Phys. J. A* **56**, 250 (2020).
3. F. Ajzenberg-Selove, “Energy levels of light nuclei $A = 5-10$,” *Nucl. Phys. A* **490**, 1–225 (1988); TUNL Nuclear Data Evaluation Project: www.tunl.duke.edu/NuclData/.
4. T. V. Shchedrina, V. Bradnova, S. Vokal, A. Vokalova, P. I. Zarubin, I. G. Zarubina, A. D. Kovalenko, A. I. Malakhov, G. I. Orlova, P. A. Rukoyatkin, V. V. Rusakova, M. Haiduc, S. P. Kharlamov, and M. M. Chernyavsky, “Peripheral interactions of relativistic ${}^{14}\text{N}$ nuclei with emulsion nuclei,” *Phys. At. Nucl.* **70**, 1230–1234 (2007); arXiv: nucl-ex/0605022.
5. A. A. Zaitsev, D. A. Artemenkov, V. Bradnova, P. I. Zarubin, I. G. Zarubina, R. R. Kattabekov, N. K. Kornegrutsa, K. Z. Mamatkulov, E. K. Mitsova, A. Neagu, P. A. Rukoyatkin, V. V. Rusakova, V. R. Sarkisyan, R. Stanoeva, M. Haiduc, and E. Firu, “Dissociation of relativistic ${}^{10}\text{B}$ nuclei in nuclear track emulsion,” *Phys. Part. Nuclei* **48**, 960–963 (2017).
6. D. A. Artemenkov, K. Z. Mamatkulov, S. P. Kharlamov, A. A. Zaitsev, and P. I. Zarubin, “Recent findings in relativistic dissociation of ${}^{10}\text{B}$ and ${}^{12}\text{C}$ nuclei,” *Few-Body Syst.* **58**, 89 (2017).

Translated by E. Baldina